

Rigorous Definition of Oxidation States of Ions in Solids

Lai Jiang, Sergey V. Levchenko, and Andrew M. Rappe*

The Makineni Theoretical Laboratories, Department of Chemistry, University of Pennsylvania, Philadelphia, Pennsylvania 19104-6323, USA

(Received 19 May 2009; revised manuscript received 14 June 2011; published 19 April 2012)

We present justification and a rigorous procedure for electron partitioning among atoms in extended systems. The method is based on wave-function topology and the modern theory of polarization, rather than charge density partitioning or wave-function projection, and, as such, reformulates the concept of oxidation state without assuming real-space charge transfer between atoms. This formulation provides rigorous electrostatics of finite-extent solids, including films and nanowires.

DOI: 10.1103/PhysRevLett.108.166403

PACS numbers: 71.15.Dx, 77.22.Ej

The concept of an oxidation state (OS) is widely used to predict chemical and spectroscopic properties of compounds, based solely on the atomic identities and the topology of their bonding [1]. For instance, the electrostatics of solids is usually described by a simple ionic model replacing atoms with point charges equal to the OS. The OS therefore plays an important role in ionic crystals whose properties are greatly influenced by electrostatics, due to the close packing of ions and the slow decay of the Coulomb interaction with distance.

Real-space electron density partitioning among atoms is a traditional way of obtaining an OS. It can also be used to approximate electrostatics and dispersion [2] in molecules and extended systems. However, with the development of wave-function-based quantum mechanics, it has become widely accepted that there is no rigorous justification for such a partitioning, due to the continuous electronic distribution. In fact, it has been demonstrated recently that the assumption about physical transfer of charge upon changing the OS is in some cases incorrect due to a “negative feedback” mechanism [3,4].

Another popular method of assigning an OS is the projection of wave functions to localized atomic orbitals [5,6], which removes the dependence on charge density. However, it suffers from dependence on the basis set and generally produces a noninteger OS. A recently proposed projection-based approach provides a way to round fractional occupation into an integer OS in metal-ligand systems and avoids the “negative feedback,” but does not work when a strong metal-metal bond is present or the ligand (electron donor) OS is desired [7].

From the examples above, it seems that there is no universal method to assign integer charges to atoms deterministically based on atomic configuration and electronic structure. Yet in another context, namely, electrolysis, ionic charge appears exactly in quanta. It has also been shown theoretically that the current associated with an atom moving in a toruslike insulator loop is due to motion of integer charges [8]. This sheds light on the idea that the OS, being a ground state property, is

measurable in a process that involves moving the atom of interest.

The question still remains of the appropriate quantity to be measured or calculated in order to evaluate the OS. While both charge density and projected occupation fail to play this role, the modern Berry phase description of polarization (or equivalently, localized Wannier functions) has been used to model interface charge [9], surface stoichiometry [10], and other properties greatly influenced by bulk electrostatics [11], making it a good candidate for further study. In fact, it has been suggested to partition electrons according to the spatial proximity of their WCs to atoms [12], but this method leaves ambiguity in determining whether a WC is adjacent to a particular nucleus.

In this Letter, we employ the ideas of quantized charge transport and modern theory of polarization to develop a rigorous methodology for distributing electrons among ions in the solid. This scheme is based solely on topology of electronic states rather than electron density. It also establishes a connection between the concepts of an oxidation state and charge quantization.

For any periodic solid, the polarization change $\Delta\vec{P}$ along an arbitrary path in a parameter space (e.g., in the space of nuclear coordinates in the adiabatic approximation) can be computed modulo $e\vec{R}/V$ (where \vec{R} is a lattice vector, and V is the volume of the unit cell) from knowledge of the system at initial and final points, provided the system remains insulating at every point of the path [13,14]. Furthermore, the uncertainty can be removed by considering smaller intervals along the path. Here, we focus our attention on a special subset of such paths, namely, the displacement of an atomic sublattice by a lattice vector \vec{R} . Since the Hamiltonian returns to itself, the polarization can change only by

$$\Delta\vec{P} = \frac{e}{V} \sum_{i=1}^3 n_i \vec{R}_i, \quad (1)$$

where n_i are integers, and \vec{R}_i are the lattice vectors defining the unit cell.

(i) Under certain conditions, $\Delta\vec{P}$ does not depend on the details of the path, as long as the system stays insulating at every point on the path. We note that it is now well established that the derivatives of polarization with respect to nuclear positions at zero applied field,

$$Z_{i,\alpha\beta}^* = V \left. \frac{\partial P_\alpha}{\partial \mathfrak{R}_{i\beta}} \right|_{\varepsilon=0}, \quad (2)$$

called Born effective charges, are gauge invariant [15]. Although the polarization \vec{P} itself is not gauge invariant, we can define the gauge-invariant change [16] in polarization $\Delta\vec{P}$ along a path C in the configuration space \mathfrak{R} as follows:

$$\Delta P_\alpha = \frac{1}{V} \sum_{i\beta} \int_C Z_{i,\alpha\beta}^* d\mathfrak{R}_{i\beta}. \quad (3)$$

The sufficient (but maybe not necessary) conditions for ΔP_α to be independent of the path are given by Stokes' theorem. Let us consider two different paths connecting two points in the configurational space. If there is at least one hypersurface bounded by the closed loop formed by these two paths, on which $Z_{i,\alpha\beta}^*$ are differentiable at every point, then, according to Stokes' theorem, the integral over the closed loop is zero, so $\Delta\vec{P}$ does not depend on the path. The Born effective charges are not differentiable in insulator-metal transition regions of the configurational space. Therefore, $\Delta\vec{P}$ is the same along any two insulating paths that can be continuously deformed to each other without crossing a metallic region.

It is interesting to note that model systems can be constructed in which the above condition is not satisfied. In such systems, a closed loop in a parameter space can result in electron transfer, leading to quantum adiabatic electron transport [14,17–19] without net nuclear current. Since we are interested in identifying ions in solids here, we limit ourselves to considering atomic displacements whose length is larger than the electron localization length, and the displacements of other atoms are all localized. This is always achievable by choosing a large enough unit cell to prevent interactions between displaced sublattices. Two insulating paths in such “dilute limit” cannot form a loop that leads to electron transfer, because electrons in an insulator are localized [20], and such electron transfer would mean that at some point on the path there would be delocalized electrons in insulating media. This is not possible without crossing the band gap and causing a metallic state on the loop. Thus, for our purposes, it is enough to find only one insulating path in parameter space. Indeed, while atoms could move in different environments along two different paths, the vacancies left behind would stay in essentially the same environment, but would have different charges during some parts of the two paths, if the charge transferred by the same atom along the two paths were different. If the system stays insulating along path 1 for

which the vacancy has a larger number of electrons, it cannot stay insulating also along path 2, because extra electrons should cross the band gap at some point along path 2.

(ii) $\Delta\vec{P}$ is parallel to \vec{R} , the lattice vector by which the sublattice is displaced. Choose a unit cell defined by \vec{R} and two other lattice vectors \vec{R}_2 and \vec{R}_3 . A supercell for the same physical crystal can be defined by lengthening the unit cell along \vec{R}_2 by a factor of m , but keeping the same dimensions along \vec{R} and \vec{R}_3 . The supercell contains the original sublattices plus their images at $k\vec{R}_2'/m$, ($k = 2, 3, \dots, m$), where $\vec{R}_2' = m\vec{R}_2$ is the new lattice vector, and the volume of the supercell is increased to $V' = mV$. If we move all of these sublattices (successively or together), the situation is equivalent to the previous one, and $\Delta\vec{P}$ is the same. But if we move one of these sublattices by \vec{R} , the new polarization change

$$\Delta\vec{P}' = \frac{e}{V'} (n'\vec{R} + n_2'\vec{R}_2' + n_3'\vec{R}_3), \quad (4)$$

must be $\Delta\vec{P}'/m$ by symmetry. Thus,

$$\begin{aligned} \Delta\vec{P}' &= \frac{e}{mV} (n'\vec{R} + mn_2'\vec{R}_2' + n_3'\vec{R}_3) \\ &= \frac{1}{m} \frac{e}{V} (n'\vec{R} + n_2\vec{R}_2 + n_3\vec{R}_3) = \frac{1}{m} \Delta\vec{P}. \end{aligned} \quad (5)$$

Since \vec{R} , \vec{R}_2 , and \vec{R}_3 are linearly independent, it immediately follows that $n' = n$, $n_2' = n_2/m$, and $n_3' = n_3$. Since n_2 must be divisible by every integer m , we get $n_2 = 0$. Similarly, we can prove that $n_3 = 0$. Therefore, displacement of a sublattice by \vec{R} creates a polarization change $\Delta\vec{P} = Ne\vec{R}/V$, directed along \vec{R} .

(iii) The quantity which we deem as oxidation state

$$N = \frac{V}{e} \frac{\Delta\vec{P} \cdot \vec{R}}{\vec{R}^2}, \quad (6)$$

is always an integer. This is evident from the conclusion of (ii): $\Delta\vec{P} = Ne\vec{R}/V$. Since polarization is proportional to the dipole moment of the unit cell, $\Delta\vec{P}$ is the change in the dipole moment upon transfer of an atom. This change is directed along the vector connecting initial and final positions of the atom, which can be interpreted as the change in dipole moment due to transfer of a constant charge Ne . Note also that according to (i), N is the same regardless of the particular path of sublattice displacement.

Moreover, in the Berry phase expression, polarization can be written in terms of Wannier function centers (WCs) [13,21]. This allows for mapping of wave functions to point charges and restoring the classic ionic model. The above conclusions then imply that transferring an atom by a lattice vector results in transferring some of the WCs by the same lattice vector, while the rest of the WCs remain in the starting unit cell. The Berry phase of the wave functions carries the information on how many WCs move

together with any particular atomic sublattice. In this framework, the physical meaning of OS defined in this method parallels the traditional definition as partitioning electrons (WCs) to atoms.

(iv) *The value of N is the same, regardless of which lattice vector \vec{R} is chosen for sublattice displacement. N in equation (6) depends only on the atomic species and its environment.* Assume a unit cell defined by \vec{R}_1 , \vec{R}_2 , and \vec{R}_3 exists, for which N along \vec{R}_1 and \vec{R}_2 are different for a given sublattice. Consider sequential displacements of the sublattice first along \vec{R}_1 , and then along \vec{R}_2 . According to the proof above, the total polarization change $\Delta\vec{P}$ should be directed along $\vec{R}_1 + \vec{R}_2$. However, since $\Delta\vec{P}$ is equal to the sum of polarization changes $\Delta\vec{P}_1$ and $\Delta\vec{P}_2$ along \vec{R}_1 and \vec{R}_2 , the total polarization change $\Delta\vec{P} = \Delta\vec{P}_1 + \Delta\vec{P}_2 = N_1 e\vec{R}_1/V + N_2 e\vec{R}_2/V$ cannot be parallel to $\vec{R}_1 + \vec{R}_2$ if N_1 and N_2 are different, hence $N_1 = N_2$.

To summarize, while the polarization for an insulator is defined modulo a quantum $e\vec{R}/V$, the *change* in polarization is well defined, and the oxidation state N of an atom determines the number of polarization quanta within this gauge-invariant change as the corresponding sublattice is moved by a lattice vector \vec{R} [22].

These four observations provide the basis for our definition of ions in solids. In the dilute limit, this formulation provides a rigorous connection between polarization and the oxidation state associated with a particular sublattice, as well as a tractable procedure for electron partitioning among the ions in a solid. The partitioning is not based on spatial proximity of WCs to a given nucleus, but is rigorously derived from the topology of electronic states. Note that the dilute limit provides a sufficient condition of the validity of (ii) to (iv), but may not be necessary.

To illustrate this new methodology, we calculate OS for atoms in ice, LiH, BaBiO₃, and Sr₂FeWO₆. We perform density functional theory calculations using the norm-conserving nonlocal pseudopotential plane wave method. The electronic structure of the first two materials is calculated with the generalized gradient approximation (GGA) to the exchange-correlation functional, as implemented in the ABINIT package [23,24]. The local density approximation (LDA) with the Hubbard U parameter, as implemented

in the QUANTUM-ESPRESSO package [25], is used to calculate the electronic structure of BaBiO₃ and Sr₂FeWO₆.

Water molecules in ice are rearranged for simplicity. Namely, each $4 \text{ \AA} \times 4 \text{ \AA} \times 3 \text{ \AA}$ tetragonal unit cell contains one water with H-O-H angle of 90° and O-H bond lengths of 1 \AA . The oxygen atom is placed at the origin, and the hydrogen atoms are on \hat{y} and \hat{z} axes.

We transfer the hydrogen atom on the \hat{z} axis to the next unit cell along \hat{z} . The path [Fig. 1(a)] consists of a 1 \AA straight line and a 1 \AA radius half circle in the H-O-H plane. N continuously increases from zero to $+1$, meaning it is H^+ , while the overall change in the perpendicular component of \vec{P} is zero.

Figure 1(b) shows $N = -2$ for the oxygen atom. In this case, the oxygen sublattice is first moved straight along the H-O-H bisector for $\sqrt{2} \text{ \AA}$, during which hydrogen atoms also move in the H-O-H plane to keep the O-H bond lengths unchanged. Next, the hydrogen atoms return to their original positions, and the oxygen atom is moved straight to the starting O location in the next unit cell.

In order to demonstrate that our formulation of the oxidation state is a function of crystal environment, we perform calculations for LiH, whose conventional OS of hydrogen is -1 . The results of calculations are shown in Fig. 1(c). LiH has the rock-salt crystal structure, with two atoms in the unit cell, and fcc lattice vectors. For each atom, the path corresponds to the transfer along one of the lattice vectors. It can be easily seen from the figure that $N = -1$ for hydrogen, revealing H^- , while for Li $N = +1$, signifying Li^+ .

Next, the BaBiO₃ system is chosen to demonstrate our method's ability to differentiate Bi^{5+} and Bi^{3+} in a single phase. The formal OS of Bi for cubic perovskite BaBiO₃ is $+4$, leading to a charge disproportionation $2\text{Bi}^{4+} \rightarrow \text{Bi}^{5+} + \text{Bi}^{3+}$ which is coupled to a collective oxygen octahedral breathing mode [26]. Therefore, a double perovskite 10-atom rhombohedral unit cell is used with a conventional lattice parameter of 8.66 \AA and octahedral breathing giving Bi-O bond lengths of 1.97 and 2.37 \AA . An effective Hubbard U term of 6 eV is applied to the oxygen $2p$ orbitals to correct for the band gap underestimation of DFT; this results in an LDA + U band gap of 1.88 eV , much larger than the published GGA band gap of 0.6 eV

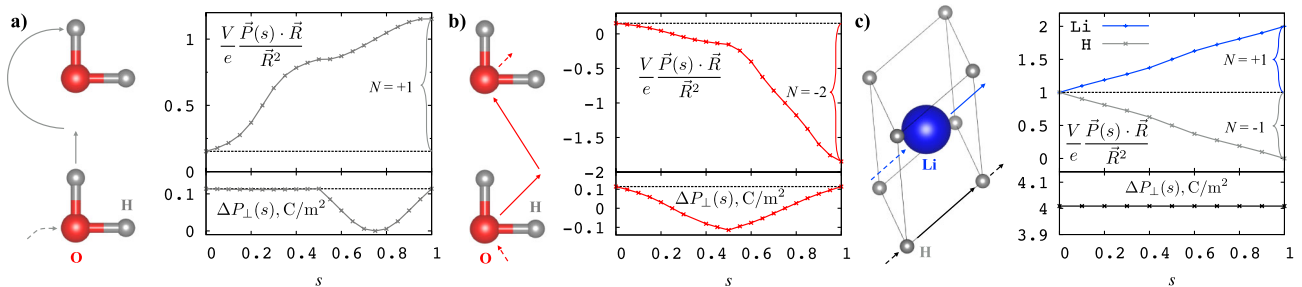


FIG. 1 (color online). Oxidation state N for hydrogen (a) or oxygen (b) in the ice model and for Li or H in LiH (c).

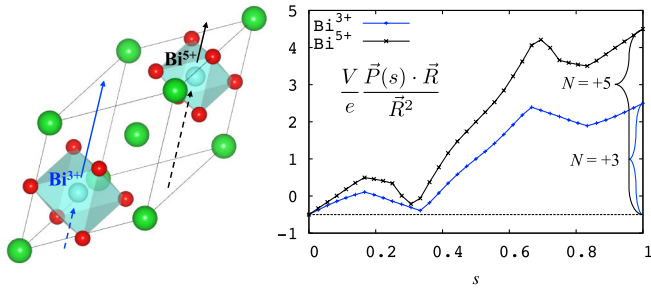


FIG. 2 (color online). Oxidation state N for the two Bi atoms in BaBiO_3 .

(with Perdew-Burke-Ernzerhof functionals) and close to the measured optical band gap of 2.05 eV [27].

Insulating paths for each Bi sublattice are found by moving the corresponding Bi cation and its images straight along a lattice vector and carefully adjusting positions of surrounding O ions to minimize Bi-O bond length change during the path. The results in Fig. 2 show that Bi in the smaller oxygen cage has $N = +5$ while the other Bi has $N = +3$, consistent with conventional wisdom that Bi^{5+} has a smaller ionic radius than Bi^{3+} .

Lastly, we use Sr_2FeWO_6 to show that for a system with variable OS elements (Fe^{2+} vs Fe^{3+}), this method can definitively assign an OS and resolve the ambiguity. While most of Sr_2FeMO_6 ($M = \text{Ta}, \text{Mo}, \text{Re}, \dots$) are ferromagnetic metals and contain Fe^{3+} , Sr_2FeWO_6 is an antiferromagnetic insulator [28]. The Fe charge state in Sr_2FeWO_6 has been studied experimentally by Mössbauer spectroscopy, and the results fall borderline between a high spin +2 and low spin +3 state. Based on the large unit cell and a purported “cancellation effect,” it is assigned to be Fe^{2+} [29]. In our calculations, we used the experimental 80-atom structure of monoclinic Sr_2FeWO_6 unit cell, which accommodates the G-type antiferromagnetic ordering of Fe [30]. An effective Hubbard U of 4 eV is added to the strongly correlated Fe 3d orbitals [31]. An Fe ion is moved along the shortest axis, and the path is initially obtained by the nudged elastic band method, with a subsequent manual adjustment of oxygen positions for bond length preservation, and the addition of more intermediate structures to ensure continuity. The result in Fig. 3 indicates that Fe has $N = +2$, as earlier work stated, and shows the ability of our methodology to identify OS for systems where ambiguity arises from multiple variable-valent elements.

To visualize the idea of “electrons topologically bound to nucleus,” we calculate the trajectories of the centers of maximally localized Wannier functions [32,33] for the H_2O system with the WANNIER90 program [34]. Figure 4(a) shows the results when the O atom is moved along the aforementioned path. Note that along the path, high symmetry structures are intentionally avoided due to the discontinuity that would otherwise occur in the trajectories. As can be seen, all WCs move with the O atom to the

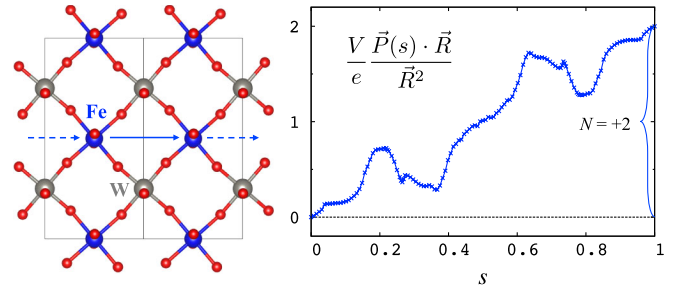


FIG. 3 (color online). Oxidation state N for Fe in Sr_2FeWO_6 .

next unit cell. The WC which we assign as the oxygen $2p_x$ orbital stays very close to the nucleus along the whole path, so that its trajectory almost coincides with the trajectory of the nucleus. WCs can also exchange their characters along the way depending on the path: the O sp^2 lone pair becomes O- H_y bond, and vice versa. When an H atom is moved, however, all WCs stay in the same unit cell [Fig. 4(b)], so that there is no overall electron displacement.

In summary, we developed a method for partitioning electrons to atoms based on their wave-function topologies. When an atom moves to its image position in periodic insulators, change of polarization reveals the number of Wannier function centers that move with the atom, provided that the system stays insulating. This effectively indicates the number of electrons that “belong” to the nucleus and establishes a rigorous definition of the oxidation state of ions in solids. This concept of “ions in solids” can have important implications for materials modeling. For example, electron redistribution upon defect formation or ion transport through a polar medium can be described

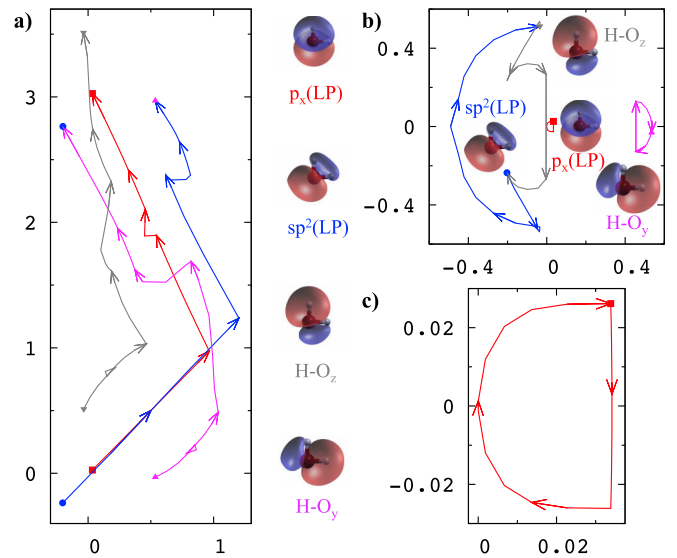


FIG. 4 (color online). Trajectories of the maximally localized WCs generated by the motion of the O (a) and H (b) in the H_2O system. The O $2p_x$ WC trajectory from (b) is shown on an expanded scale in (c). The units are Å.

in terms of ion deformation (no change in OS) or charge transfer (when OS changes).

L.J. was supported by the US AFOSR under Grant No. FA9550-10-1-0248, S. V.L. was supported by the US DOE BES under Grant No. DE-FG02-07ER15920, and A.M.R. was supported by the US ONR under Grant No. N00014-11-1-0578. Computational support was provided by the US DOD. We thank Eugene J. Mele, Barri J. Gold and Ilya Grinberg for fruitful discussions.

*rappe@sas.upenn.edu

- [1] C. K. Jørgensen, *Oxidation Numbers and Oxidation States* (Springer-Verlag, New York Inc., 1969).
- [2] A. Tkatchenko and M. Scheffler, *Phys. Rev. Lett.* **102**, 073005 (2009).
- [3] R. Resta, *Nature (London)* **453**, 735 (2008).
- [4] H. Raebiger, S. Lany, and A. Zunger, *Nature (London)* **453**, 763 (2008).
- [5] P. O. Lowdin, *J. Chem. Phys.* **18**, 365 (1950).
- [6] R. S. Mulliken, *J. Chem. Phys.* **23**, 1833 (1955).
- [7] P. H.-L. Sit, R. Car, M. H. Cohen, and A. Selloni, *Inorg. Chem.* **50**, 10259 (2011).
- [8] J. B. Pendry and C. H. Hodges, *J. Phys. C* **17**, 1269 (1984).
- [9] N. C. Bristowe, P. B. Littlewood, and E. Artacho, *J. Phys. Condens. Matter* **23**, 081001 (2011).
- [10] S. V. Levchenko and A. M. Rappe, *Phys. Rev. Lett.* **100**, 256101 (2008).
- [11] C. Noguera, *J. Phys. Condens. Matter* **12**, R367 (2000).
- [12] P. H.-L. Sit, F. Zipoli, J. Chen, R. Car, M. H. Cohen, and A. Selloni, *Chem. Eur. J.* **17**, 12136 (2011).
- [13] R. D. King-Smith and D. Vanderbilt, *Phys. Rev. B* **47**, 1651 (1993).
- [14] D. Vanderbilt and R. D. King-Smith, *Phys. Rev. B* **48**, 4442 (1993).
- [15] R. Resta, *Rev. Mod. Phys.* **66**, 899 (1994).
- [16] K. M. Rabe and U. V. Waghmare, *Ferroelectrics* **136**, 147 (1992).
- [17] D. J. Thouless, *Phys. Rev. B* **27**, 6083 (1983).
- [18] Q. Niu, *Phys. Rev. B* **34**, 5093 (1986).
- [19] Q. Niu, *Phys. Rev. Lett.* **64**, 1812 (1990).
- [20] E. I. Blount, in *Solid State Physics: Advances in Research and Applications*, edited by F. Seitz and D. Turnbull (Academic Press, New York, 1962), Vol. 13, pp. 305–73.
- [21] J. Zak, *Phys. Rev. Lett.* **62**, 2747 (1989).
- [22] See Supplemental Material at <http://link.aps.org/supplemental/10.1103/PhysRevLett.108.166403> for graphical illustration of sublattice displacement.
- [23] X. Gonze, B. Amadon, P.-M. Anglade, J.-M. Beuken, F. Bottin, P. Boulanger, F. Bruneval, D. Caliste, R. Caracas, M. Cote *et al.*, *Comput. Phys. Commun.* **180**, 2582 (2009).
- [24] X. Gonze, G.-M. Rignanese, M. Verstraete, J.-M. Beuken, Y. Pouillon, R. Caracas, F. Jollet, M. Torrent, G. Zerah, M. Mikami *et al.*, *Z. Kristallogr.* **220**, 558 (2005).
- [25] P. Giannozzi, S. Baroni, N. Bonini, M. Calandra, R. Car, C. Cavazzoni, D. Ceresoli, G. L. Chiarotti, M. Cococcioni, I. Dabo *et al.*, *J. Phys. Condens. Matter* **21**, 395502 (2009).
- [26] T. Thonhauser and K. M. Rabe, *Phys. Rev. B* **73**, 2121061 (2006).
- [27] J. Tang, Z. Zou, and J. Ye, *J. Phys. Chem. C* **111**, 12779 (2007).
- [28] H. Kawanaka, I. Hase, S. Toyama, and Y. Nishihara, *J. Phys. Soc. Jpn.* **68**, 2890 (1999).
- [29] H. Kawanaka, S. T. I. Hase, and Y. Nishihara, *Physica B (Amsterdam)* **281-282**, 518 (2000).
- [30] S. DiMatteo, G. Jackeli, and N. B. Perkins, *Phys. Rev. B* **67**, 184427 (2003).
- [31] Z. Fang, K. Terakura, and J. Kanamori, *Phys. Rev. B* **63**, 180407 (2001).
- [32] N. Marzari and D. Vanderbilt, *Phys. Rev. B* **56**, 12847 (1997).
- [33] S. F. Boys, *Rev. Mod. Phys.* **32**, 296 (1960).
- [34] A. A. Mostofi, J. R. Yates, Y.-S. Lee, I. Souza, D. Vanderbilt, and N. Marzari, *Comput. Phys. Commun.* **178**, 685 (2008).